

Coulomb chronometry to probe the decay mechanism of hot nuclei

D. Gruyer,^{1,*} J.D. Frankland,^{1,†} E. Bonnet,¹ A. Chbihi,¹ G. Ademard,² M. Boisjoli,^{1,3} B. Borderie,² R. Bougault,⁴ E. Galichet,^{2,5} J. Gauthier,³ D. Guinet,⁶ P. Lantesse,⁶ N. Le Neindre,⁴ E. Legouée,⁴ O. Lopez,⁴ L. Manduci,⁷ P. Marini,¹ K. Mazurek,⁸ P.N. Nadtochy,⁹ M. Pârlog,^{4,10} M. F. Rivet,² R. Roy,³ E. Rosato,^{11,12} G. Spadaccini,^{11,12} G. Verde,¹³ E. Vient,⁴ M. Vigilante,^{11,12} and J.P. Wieleczko¹

(INDRA collaboration)

¹*GANIL, CEA-DSM/CNRS-IN2P3, Bvd. Henri Becquerel, F-14076 Caen CEDEX, France*

²*Institut de Physique Nucléaire, CNRS/IN2P3, Université Paris-Sud 11, F-91406 Orsay CEDEX, France*

³*Département de physique, de génie physique et d'optique, Université Laval, Québec, G1V 0A6 Canada*

⁴*LPC, CNRS/IN2P3, Ensicaen, Université de Caen, F-14050 Caen CEDEX, France*

⁵*Conservatoire National des Arts et Métiers, F-75141 Paris Cedex 03, France*

⁶*Institut de Physique Nucléaire, Université Claude Bernard Lyon 1,*

CNRS/IN2P3, F-69622 Villeurbanne CEDEX, France

⁷*École des Applications Militaires de l'énergie Atomique, B.P. 19, F-50115 Cherbourg, France*

⁸*H. Niewodniczański Institute of Nuclear Physics, PL-31342 Kraków, Poland*

⁹*Omsk State University, Mira prospekt 55-A, Omsk 644077, Russia*

¹⁰*National Institute for Physics and Nuclear Engineering, RO-077125 Bucharest-Măgurele, Romania*

¹¹*Dipartimento di Fisica, Università degli Studi di Napoli FEDERICO II, I-80126 Napoli, Italy*

¹²*Istituto Nazionale di Fisica Nucleare, Sezione di Napoli,*

Complesso Universitario di Monte S. Angelo, Via Cintia Edificio 6, I-80126 Napoli, Italy

¹³*Istituto Nazionale di Fisica Nucleare, Sezione di Catania, 64 Via Santa Sofia, I-95123, Catania, Italy*

In $^{129}\text{Xe}+^{nat}\text{Sn}$ central collisions from 12 to 25 MeV/A, the three-fragment exit channel occurs with a significant cross section. We show that these fragments arise from two successive binary splittings of a heavy composite system. The sequence of fragment production is unambiguously determined. Strong Coulomb proximity effects are observed in the three-fragment final state. A comparison with Coulomb trajectory calculations shows that the time scale between the consecutive break-ups decreases with increasing bombarding energy, becoming quasi-simultaneous above excitation energy $E^* = 4.0 \pm 0.5$ MeV/A.

PACS numbers: 25.70.-z, 25.70.Jj, 25.70.Pq, 06.30.Ft

Introduction. In heavy ion collisions at bombarding energies around 10 – 20 MeV/A, namely well above the Coulomb barrier but below the Fermi energy regime, different types of reaction mechanism are expected. The final state can result from the production of one, two, three, or more heavy fragments. By detecting all of them in coincidence and correlating their mass (charge), energy, and momentum one is able to better understand the underlying reaction and decay mechanisms. However, when the final state is composed of more than two fragments, few experimental data are available [1–3] leaving room for ambiguities in the correct interpretation of the reaction mechanism. New theoretical efforts are made to cover this energy range including time dependent microscopic approaches [4, 5], transport models [6] and molecular dynamics calculations [7].

Recent data on $^{129}\text{Xe}+^{nat}\text{Sn}$ central collisions [8] show that at 8 MeV/A bombarding energy, almost all the reaction cross section is composed of events with two heavy fragments in the exit channel (see Fig.1(a)). Above 12 MeV/A bombarding energy, the three-fragment exit channel becomes significant, overcoming the two-fragment production cross section above 18 MeV/A. The decay mechanism responsible for these three-fragment events is not well established: Is it the continuation of low

energy fission or the precursor of high energy simultaneous fragmentation? To answer this question, a dynamical characterization of the decay mechanism is needed. In particular, the estimation of the involved time scales may allow to disentangle sequences of two binary fission from simultaneous three-fragment break-up. This information is of great importance in the view of constructing reaction models with predictive power in this energy regime.

Several methods have been proposed for time scale measurement in peripheral heavy-ion collisions [2, 9, 10]. Such methods were recently used to probe the isospin equilibration between projectile and target nuclei [11–14]. However, they are not suitable for central collisions, where the fragments arise from the decay of an excited composite system.

In the case of central collisions, two-fragment correlation functions have been used to extract emission time scales in multifragmentation events, typically observed at intermediate energies [15–19]. The extracted emission properties are affected by space-time ambiguities. Moreover, distortions of the correlation function's shape induced by momentum and energy conservation laws [20], collective motion and reaction plane orientation effects [21, 22], while small or negligible in the case of light particle correlation studies, may become important

and difficult to deal with in the case of massive fragment-fragment correlations [17].

In this letter, we propose a new Coulomb chronometer suitable for three-fragment exit channels. The proposed method is based on the unambiguous identification of the sequence of fragment production, which partially removes the space-time ambiguity inherent in commonly adopted correlation function techniques. In addition, this method is not affected by possible distortions induced by conservation laws, since it fully takes into account the overall balance of charge, energy and momentum. We use this chronometer to extract the evolution of the fragment emission time in $^{129}\text{Xe}+^{nat}\text{Sn}$ central collisions from 12 to 25 MeV/A bombarding energy.

Experimental analysis. Collisions of $^{129}\text{Xe}+^{nat}\text{Sn}$ at 12, 15, 18, 20, and 25 MeV/A were measured using the INDRA 4π charged product array [23] at the GANIL accelerator facility. This detector, composed of 336 detection cells arranged in 17 rings centered on the beam axis, covers 90% of the solid angle and can identify in charge fragments from hydrogen to uranium with low thresholds. In this analysis, we considered only fusion-like events leading to three heavy fragments ($Z > 10$) in the exit channel. To select the fusion-like events, we have used the kinematic global variable proposed in [24], but here applied to the sum of the three heaviest fragments. The selected events correspond to an average total detected charge ranging from $\langle Z_{tot} \rangle = 96$ at 12 MeV/A to $\langle Z_{tot} \rangle = 91$ at 25 MeV/A. Therefore the probability to miss a heavy fragment is very low.

We start from the hypothesis that fragments are produced sequentially. If two successive splittings occur, three possible sequences of splittings have to be considered. To identify the sequence of splittings event by event, we compare the relative velocity between each pair of fragments with that expected for fission, taken from the Viola systematics [25, 26]. The pair with the most Viola-like relative velocity is considered to have been produced during the second splitting. We can therefore trivially deduce that the remaining fragment was emitted first. This procedure amounts to computing, for each event, the three following quantities:

$$\chi_i = (v_{jk}^{exp} - v_{jk}^{viola})^2,$$

with $i = 1, 2, 3$ the index of the fragment produced in the first splitting and v_{jk} the relative velocity between the remaining two fragments. The smallest value of χ_i determines the sequence of splittings. This minimisation procedure is inspired by that proposed by Bizard et al. in [27].

Once the sequence of splittings is known event by event, fragments can be sorted according to their order of production and the intermediate system can be reconstructed. The charge of the incomplete fusion source Z_{src} is obtained by summing the three detected fragments. Let us now call Z_1^f and Z_2^f , the two nuclei coming from

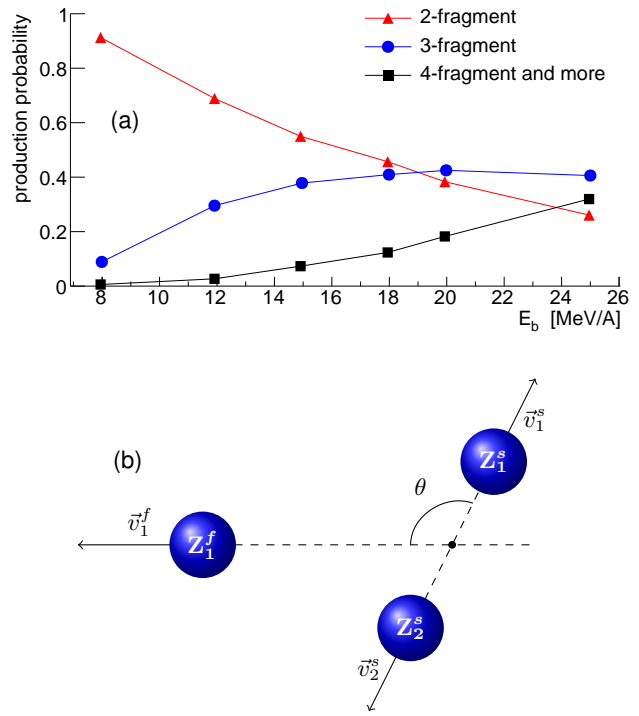


Figure 1: (color online). (a) Evolution of different exit channel probabilities as a function of the beam energy for $^{129}\text{Xe}+^{nat}\text{Sn}$ central collisions. (b) Definition of the relevant kinematic observables for the three-fragment exit channel, in the rest frame of the intermediate system Z_2^f .

the first splitting. The fragment Z_2^f breaks later in Z_1^s and Z_2^s (see Fig.1(b)). Mean charges and charge asymmetries $\langle \delta Z \rangle = \langle (Z_2 - Z_1)/(Z_2 + Z_1) \rangle$ of the two splittings are presented in Tab.I. The mean charge asymmetry of the first splitting $\langle \delta Z^f \rangle$ is significantly larger than the quasi-symmetric entrance channel. It is a strong indication that the first stage of the reactions is an incomplete fusion of projectile and target nuclei, leading to the formation of heavy composite systems with atomic numbers at least as large as the values of $\langle Z_{src} \rangle$ presented in Tab.I (no attempt was made to correct fragment charges for pre- or post-scission evaporation of charged particles).

We now characterize the two splittings by their relative orientation. Fig.2 shows the evolution of the anisotropy ($W(0^\circ)/W(90^\circ)$) of the distribution of the angle, θ , between the two separation axes (see Fig.1(b)) as a function of the beam energy. At the lowest beam energies, the angular distribution presents a “U” shape (inset of Fig.2) which is characteristic of fission of an equilibrated system [28] with angular momentum. With increasing beam energy, the angular distribution flattens ($W(0^\circ)/W(90^\circ) = 1$) and then shows a maximum centered on $\theta \sim 90^\circ$ (inset of Fig.2), leading to an anisotropy lower than 1. Such an anisotropy is unexpected for an isolated fissioning system and suggests the presence of a

	$\langle Z_{src} \rangle$	$\langle Z_1^f \rangle$	$\langle Z_2^f \rangle$	$\langle \delta Z^f \rangle$	$\langle Z_1^s \rangle$	$\langle Z_2^s \rangle$	$\langle \delta Z^s \rangle$
12 MeV/A	88.8	25.5	63.3	0.44	40.0	23.3	0.26
15 MeV/A	84.0	24.5	59.7	0.43	38.2	21.5	0.28
18 MeV/A	79.9	24.0	55.8	0.41	35.8	20.0	0.28
20 MeV/A	76.0	23.7	52.2	0.40	33.3	18.9	0.27
25 MeV/A	69.5	23.6	45.9	0.32	28.9	17.4	0.25
E.C.	104	50	54	0.04	-	-	-

Table I: Mean charges and charge asymmetries of the two splittings for $^{129}\text{Xe}+^{nat}\text{Sn}$ central collisions. Z_{src} is the charge of the reconstructed incomplete fusion source and the exponent f (s) stands for the first (second) splitting. E.C. refers to the entrance channel.

Coulomb final state interaction, where the Coulomb field of the first emitted fragment focalises the other two more perpendicularly to the first separation axis. Without going into a detailed discussion of the Coulomb final state interaction, it is clear at this point that the presence of such an anisotropy requires the second splitting to take place at a distance from the first emitted fragment of the same order of magnitude as the distance between the center of the fissioning fragments at scission.

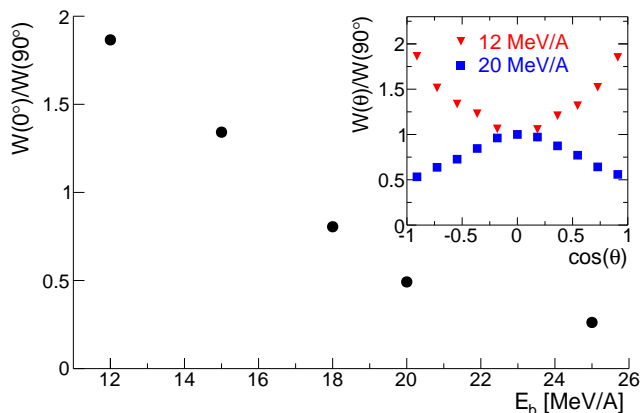


Figure 2: (color online). Anisotropy of the distribution of the inter-splitting angle, $W(0^\circ)/W(90^\circ)$, as a function of the beam energy for $^{129}\text{Xe}+^{nat}\text{Sn}$ central collisions. Angular distributions obtained at beam energies of 12 MeV/A (red triangle) and 20 MeV/A (blue squares) are shown in the inset. Statistical error bars are smaller than the size of the points.

To estimate the mean inter-splitting time, we used the correlation between the inter-splitting angle θ and the relative velocity of the second splitting: $v_{12}^s = \|\vec{v}_1^s - \vec{v}_2^s\|$ (see Fig.1(b)). In fact, for long inter-splitting times the second splitting occurs far from the first emitted fragment. The relative velocity v_{12}^s is then only determined by the mutual repulsion between Z_1^s and Z_2^s and should not depend on the relative orientation of the two splittings. However, for short inter-splitting time the second splitting occurs close to the first emitted fragment. The relative velocity v_{12}^s is modified by the Coulomb field of

Z_1^f and depends on the relative orientation of the two splittings. In this case, v_{12}^s should present a maximum for $\theta = 90^\circ$. We used this Coulomb proximity effect as a chronometer to measure the inter-splitting time δt .

The experimental correlation between v_{12}^s and θ is presented in Fig.3(a), for all beam energies. These correlations present a maximum at $\theta \sim 90^\circ$, which is more pronounced as the beam energy increases. We quantify this effect by the Coulomb distortion parameter $\delta v = v_{12}^s(90^\circ) - v_{12}^s(0^\circ)$. δv increases with the beam energy (Fig.3(b)), indicating that the second splitting occurred closer and closer to the first emitted fragment.

To translate δv in terms of inter-splitting time δt , we performed Coulomb trajectory calculations for punctual charges, which simulate sequential break-ups using mean charges given in Tab.I. The initial conditions of the calculation were chosen in order to reproduce the systematics of asymmetric fission [26]: for each step the two fissioning fragments were separated by a distance $d_{ij} = r_0(A_i^{1/3} + A_j^{1/3})$ with $r_0 = 1.9$ fm. δv is then computed by varying δt . Finally, we obtained the evolution of the inter-splitting time as a function of the beam energy (Fig.4). The vertical error bars in Fig.4 reflect the statistical uncertainties on the measurement of δv (Fig.3(b)) and take into account variations of the initial conditions in the trajectory calculations ($r_0 = 1.9 - 1.5$ fm). We verified that the experimental apparatus does not introduce significant systematic errors on the average values.

Results. A clear decrease of the inter-splitting time with increasing beam energy is observed in Fig.4. At 12 MeV/A, the inter-splitting time δt is of the order of 500 fm/c. It shows that, for the lower beam energies, fragments arise from two successive splittings, validating our starting hypothesis. As the beam energy increases from 12 MeV/A to 20 MeV/A, δt decreases monotonically from 500 fm/c to about 100 fm/c. Above 20 MeV/A, δt becomes very short and saturates below 100 fm/c. This saturation of the fragment emission time has been interpreted as evidence for simultaneous multifragmentation [16, 29, 30], but it reflects here the sensitivity limit of the method. Indeed, our trajectory calculations show that below $\delta t \sim 100$ fm/c the two nuclei resulting from the first splitting do not have sufficient time to move apart beyond the range of the nuclear forces before the second splitting occurs. For such a short time, fragment emissions can not be treated independently, and it is no longer meaningful to speak of a sequential process. This inter-splitting time is reached around 20 MeV/A.

Discussion. Our results show that the three-fragment exit channel is compatible with successive binary splittings on shorter and shorter time scales, becoming indistinguishable from simultaneous three-fragment break-up

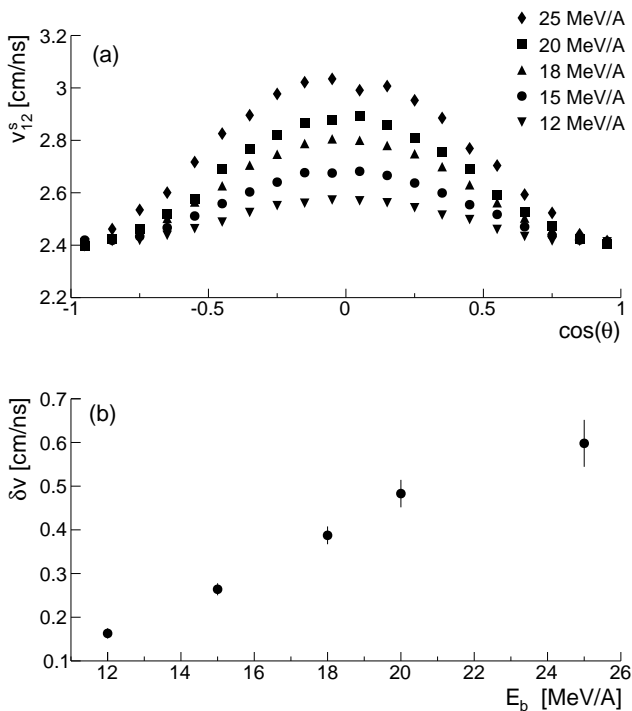


Figure 3: (a) Correlation between the inter-splitting angle θ and the relative velocity of the second splitting v_{12}^s , vertical error bars are smaller than the size of the points; (b) evolution of the Coulomb distortion parameter δv as a function of the beam energy for $^{129}\text{Xe}+^{nat}\text{Sn}$ central collisions.

at bombarding energies above 20 MeV/A. For each beam energy, the excitation energy of the initial compound system formed by incomplete fusion has been estimated using a standard calorimetric procedure [31–33], including the light charged particles detected in coincidence. The mean values are given in the upper scale of Fig.4. It can be seen that the excitation energy above which the three-fragment production becomes quasi-simultaneous is $E^* \sim 4$ MeV/A. Our results are in agreement with fragment emission times extracted for excited gold nuclei formed in $\pi^- + Au$ reactions [16] over the whole excitation energy range. Break-up times for similar-sized nuclei formed in heavy-ion induced reactions [34–36] show the same trend, but time scales for excitation energies below 5 MeV/A are systematically larger than those of [16], and measurements from different reactions give widely varying results. This discrepancy can be due to angular momentum or compression-expansion effects which are negligible in hadron induced reaction [16] but depend on the entrance channel in heavy-ion collisions [33]. This issue could be fixed with a systematic study of fragment emission times over a broad range of excitation energy and system size, and also by extending the presented method to more than three-fragment exit channel.

Conclusion. In summary, we proposed a new chronometer which takes advantage of Coulomb prox-

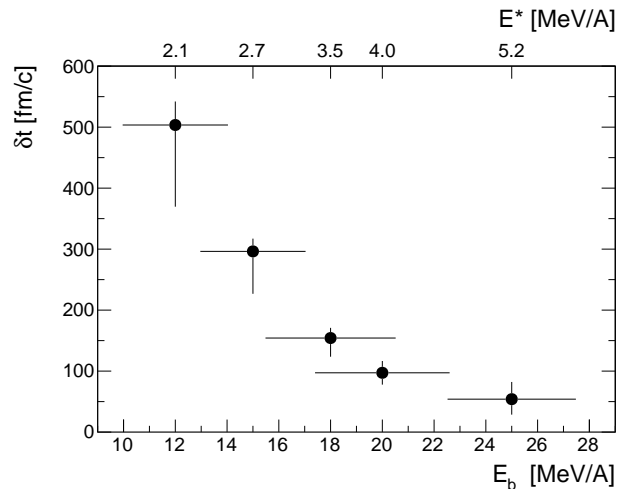


Figure 4: Evolution of the mean inter-splitting time δt as a function of the beam energy (lower scale) and the estimated excitation energy of the incomplete fusion source (upper scale) produced in $^{129}\text{Xe}+^{nat}\text{Sn}$ central collisions. Horizontal error bars refer to the upper scale.

imity effects observed in the three-fragment final state. This is made possible thanks to the highly exclusive measurement performed with INDRA. The originality of the method relies on the unambiguous determination of the sequence of splitting. This method is applied to probe the decay mechanism responsible for the three-fragment exit channel observed in $^{129}\text{Xe}+^{nat}\text{Sn}$ central collisions at bombarding energies from 12 to 25 MeV/A. We showed that these fragments arise from successive binary splittings occurring on shorter and shorter time scales. The involved time scale becomes compatible with simultaneous three-fragment break-up above $E^* = 4.0 \pm 0.5$ MeV/A, which can be interpreted as the signature of the onset of multifragmentation.

The authors would like to thank Dominique Durand for useful discussions and the staff of the GANIL Accelerator facility for their continued support during the experiments. D. G. gratefully acknowledges the financial support of the Commissariat à l'énergie Atomique and the Conseil Régional de Basse-Normandie. The work was partially sponsored by the French-Polish agreements IN2P3-COPIN (Project No. 09-136) and the Russian Foundation for Basic Research, Research Project No. 13-02-00168 (Russia).

* Electronic address: diego.gruyer@ganil.fr

† Electronic address: john.frankland@ganil.fr

[1] R. J. Charity, R. Freifelder, A. Gobbi, N. Herrmann, K. D. Hildenbrand, F. Rami, H. Stelzer, J. P. Wessels, G. Casini, P. R. Maurenzig, et al., *Zeitschrift für Physik*

- A Hadrons and Nuclei **341**, 53 (1991).
- [2] G. Casini, P. G. Bizzeti, P. R. Maurenzig, A. Olmi, A. A. Stefanini, J. P. Wessels, R. J. Charity, R. Freifelder, A. Gobbi, N. Herrmann, et al., *Physical Review Letters* **71**, 2567 (1993).
- [3] J. Wilczyński, I. Skwira-Chalot, K. Siwek-Wilczyńska, A. Pagano, F. Amorini, A. Anzalone, L. Auditore, V. Baran, J. Brzychczyk, G. Cardella, et al., *Physical Review C* **81**, 024605 (2010).
- [4] C. Golabek and C. Simenel, *Physical Review Letters* **103**, 042701 (2009).
- [5] K. Sekizawa and K. Yabana, *Physical Review C* **88**, 014614 (2013).
- [6] E. G. Ryabov, A. V. Karpov, P. N. Nadtochy, and G. D. Adeev, *Physical Review C* **78**, 044614 (2008).
- [7] Y. Li, S. Yan, X. Jiang, and L. Wang, *Nuclear Physics A* **902**, 1 (2013).
- [8] A. Chbihi, L. Manduci, J. Moisan, E. Bonnet, J. D. Frankland, R. Roy, and G. Verde, *Journal of Physics: Conference Series* **420**, 012099 (2013).
- [9] A. A. Stefanini, G. Casini, P. R. Maurenzig, A. Olmi, R. J. Charity, R. Freifelder, A. Gobbi, N. Herrmann, K. D. Hildenbrand, M. Petrovici, et al., *Zeitschrift für Physik A Hadrons and Nuclei* **351**, 167 (1995).
- [10] E. De Filippo, A. Pagano, J. Wilczyński, F. Amorini, A. Anzalone, L. Auditore, V. Baran, I. Berceanu, J. Blicharska, J. Brzychczyk, et al., *Physical Review C* **71**, 044602+ (2005).
- [11] A. B. McIntosh, S. Hudan, J. Black, D. Mercier, C. J. Metelko, R. Yanez, R. T. de Souza, A. Chbihi, M. Famiano, M. O. Frégeau, et al., *Physical Review C* **81**, 034603+ (2010).
- [12] S. Hudan, A. B. McIntosh, R. T. de Souza, S. Bianchin, J. Black, A. Chbihi, M. Famiano, M. O. Frégeau, J. Gauthier, D. Mercier, et al., *Physical Review C* **86**, 021603+ (2012).
- [13] K. Brown, S. Hudan, R. T. deSouza, J. Gauthier, R. Roy, D. V. Shetty, G. A. Souliotis, and S. J. Yennello, *Physical Review C* **87**, 061601 (2013).
- [14] E. De Filippo, A. Pagano, P. Russotto, F. Amorini, A. Anzalone, L. Auditore, V. Baran, I. Berceanu, B. Borderie, R. Bougault, et al., *Physical Review C* **86**, 014610+ (2012).
- [15] D. Durand, *Nuclear Physics A* **630**, 52 (1998).
- [16] L. Beaulieu, T. Lefort, K. Kwiatkowski, R. T. de Souza, Hsi, L. Pienkowski, B. Back, D. S. Bracken, H. Breuer, E. Cornell, et al., *Physical Review Letters* **84**, 5971 (2000).
- [17] G. Verde, A. Chbihi, R. Ghetti, and J. Helgesson, *The European Physical Journal A - Hadrons and Nuclei* **30**, 81 (2006).
- [18] G. Tăbăcaru, M.-F. Rivet, B. Borderie, M. Pârlog, B. Bouriquet, A. Chbihi, J. Frankland, J. Wieleczko, E. Bonnet, R. Bougault, et al., *Nuclear Physics A* **764**, 371 (2006).
- [19] B. Borderie and M.-F. Rivet, *Progress in Particle and Nuclear Physics* **61**, 551 (2008).
- [20] Z. Chajęcki and M. Lisa, *Physical Review C* **78**, 064903 (2008).
- [21] B. Kämpfer, R. Kotte, J. Mösner, W. Neubert, D. Wohlfarth, J. P. Alard, Z. Basrak, N. Bastid, I. M. Belayev, T. Blaich, et al., *Physical Review C* **48**, R955 (1993).
- [22] G. Verde, P. Danielewicz, W. G. Lynch, C. F. Chan, C. K. Gelbke, L. K. Kwong, T. X. Liu, X. D. Liu, D. Seymour, R. Shomin, et al., *Physics Letters B* **653**, 12 (2007).
- [23] J. Pouthas, B. Borderie, R. Dayras, E. Plagnol, M.-F. Rivet, F. Saint-Laurent, J. C. Steckmeyer, G. Auger, C. O. Bacri, S. Barbey, et al., *Nuclear Instruments and Methods in Physics Research Section A: Accelerators, Spectrometers, Detectors and Associated Equipment* **357**, 418 (1995).
- [24] M. Kabtoul, Ph.D Thesis, Université de Caen-Basse Normandie (2013).
- [25] V. E. Viola, K. Kwiatkowski, and M. Walker, *Physical Review C* **31**, 1550 (1985).
- [26] D. Hinde, J. Leigh, J. Bokhorst, J. Newton, R. Walsh, and J. Boldeman, *Nuclear Physics A* **472**, 318 (1987).
- [27] G. Bizard, D. Durand, A. Genoux-Lubain, M. Louvel, R. Bougault, R. Brou, H. Doubre, Y. El-Masri, H. Fugiwara, K. Hagel, et al., *Physics Letters B* **276**, 413 (1992).
- [28] S. E. Vigdor, H. J. Karwowski, W. W. Jacobs, S. Kailas, P. P. Singh, F. Soga, and P. Yip, *Physics Letters B* **90**, 384 (1980).
- [29] E. Bauge, A. Elmaani, R. A. Lacey, J. Lauret, N. N. Ajitanand, D. Craig, M. Cronqvist, E. Gualtieri, S. Hanuschke, T. Li, et al., *Physical Review Letters* **70**, 3705 (1993).
- [30] Z. Y. He, L. Gingras, Y. Larochelle, D. Ouerdane, L. Beaulieu, P. Gagné, X. Qian, R. Roy, C. St Pierre, G. C. Ball, et al., *Physical Review C* **63**, 011601+ (2000).
- [31] D. Cussol, G. Bizard, R. Brou, D. Durand, M. Louvel, J. Patry, J. Peter, R. Regimbart, J. C. Steckmeyer, and J. Sullivan, *Nuclear Physics A* **561**, 298 (1993).
- [32] N. Marie, R. Laforest, R. Bougault, J. Wieleczko, D. Durand, C. Bacri, J. Lecolley, F. Saint-Laurent, G. Auger, J. Benlliure, et al., *Physics Letters B* **391**, 15 (1997).
- [33] E. Bonnet, B. Borderie, N. L. Neindre, M.-F. Rivet, R. Bougault, A. Chbihi, R. Dayras, J. Frankland, E. Galichet, F. Gagnon-Moisan, et al., *Nuclear Physics A* **816**, 1 (2009).
- [34] R. Bougault, J. Colin, F. Delaunay, A. Genoux-Lubain, A. Hajfani, C. Le Brun, J. F. Lecolley, M. Louvel, and J. C. Steckmeyer, *Physics Letters B* **232**, 291 (1989).
- [35] M. Louvel, A. Genoux-Lubain, G. Bizard, R. Bougault, R. Brou, A. Buta, H. Doubre, D. Durand, Y. El Masri, H. Fugiwara, et al., *Physics Letters B* **320**, 221 (1994).
- [36] D. Durand, J. Colin, J. F. Lecolley, C. Meslin, M. Aboufirassi, B. Bilwes, R. Bougault, R. Brou, F. Cosmo, J. Galin, et al., *Physics Letters B* **345**, 397 (1995).